SAND2015-2688C

Dehydration of Uranyl Nitrate Hexahydrate to the Trihydrate under Ambient Conditions as Observed via Dynamic Infrared Reflectance Spectroscopy

Timothy J. Johnson[a], Lucas E. Sweet[a], David E. Meier[a], Edward J. Mausolf[a], Eunja Kim[b],
Philippe F. Weck[c], Edgar C. Buck[a] and Bruce K. McNamara[a]

[a]Pacific Northwest National Laboratory, P.O. Box 999, Richland, WA, USA 99354;
[b]Department of Physics and Astronomy, University of Nevada Las Vegas,
4505 Maryland Parkway, Las Vegas, Nevada USA, 89154
[c]Sandia National Laboratories, P.O. Box 5800, MS 0779, Albuquerque, New Mexico USA 87185

ABSTRACT

Uranyl nitrate is a key species in the nuclear fuel cycle, but is known to exist in different states of hydration, including the hexahydrate [$UO_2(NO_3)_2(H_2O)_6$] and the trihydrate [$UO_2(NO_3)_2(H_2O)_3$] forms. Their stabilities depend on both relative humidity and temperature. Both phases have been previously studied by infrared transmission spectroscopy, but the data were limited both by both instrumental resolution and the ability to prepare the samples as pellets without desiccating it. We report time-resolved infrared measurements using an integrating sphere that allow us to observe transformation from the hexahydrate to the trihydrate simply by flowing dry nitrogen gas over the sample. Hexahydrate samples were prepared and confirmed via known XRD patterns then measured in reflectance mode; the hexahydrate has a distinct uranyl asymmetric stretch band at 949.0 cm^{-1} that shifts to shorter wavelengths and broadens as the sample dehydrates and recrystallizes to the trihydrate, first as a blue edge shoulder but ultimately resulting in a doublet band with reflectance peaks at 966 and 957 cm^{-1}. The data are consistent with transformation from UNH to UNT since UNT has two non-equivalent UO_2^{2+} sites. The dehydration of $UO_2(NO_3)_2(H_2O)_6$ to $UO_2(NO_3)_2(H2O)_3$ is both a morphological and structural change that has the lustrous lime green crystals changing to the dull greenish yellow of the trihydrate. Crystal structures and phase transformation were confirmed theoretically using DFT calculations and experimentally via microscopy methods. Both methods showed a transformation with two distinct sites for the uranyl cation in the trihydrate, as opposed to a single crystallographic site in the hexahydrate.

Keywords: uranyl nitrate, uranyl nitrate hexahydrate, infrared spectroscopy, microscopy, reflectance spectroscopy, reststrahlen bands, density functional theory.

1. INTRODUCTION

Uranyl nitrate is a key species in the uranium fuel cycle as it is occurs at several stages of the cycle. After the milling and extraction steps to produce uranium ore concentrate (UOC, also sometimes known as yellowcake), the UOC is reacted with nitric acid to produce uranyl nitrate, which often precipitates in the hexahydrate form. Depending on the process used, this material is subsequently calcined to make UO_2, which is later converted with fluorine compounds for the enrichment processes. Uranyl nitrate is also a key component in the reprocessing steps, i.e. in those processes where spent fuel is re-dissolved in acid (ultimately resulting in the precipitation of UNH) to be reintroduced to the enrichment steps. One important aspect of uranyl nitrate is that it is one of the most water-soluble components in the uranium fuel cycle. In the solid phase the nitrate is known to exist in different states of hydration, including the hexahydrate [$UO_2(NO_3)_2(H_2O)_6$] and trihydrate [$UO_2(NO_3)_2(H_2O)_3$] forms, and in extremely dry environs even as the dihydrate [$UO_2(NO_3)_2(H_2O)_2$]. The relative stabilities of these species depend on both water vapor pressure and temperature. More than a half-century ago, these various hydrates were all studied by infrared transmission spectroscopy, but were limited both by the instrumental resolution of the day and (we surmise) by the inability to prepare the samples as transmission mulls or pellets without affecting the sample. In this stud we use an alternate method that does not require pellet preparation (and we suspect desiccation of the material). Instead we employ time-resolved infrared spectroscopy in reflectance mode. This technique requires no sample preparation; it places the sample at the port of an integrating sphere that allows one to observe the transformation from the hexahydrate to the trihydrate simply by flowing a stream of dry nitrogen gas over the sample. As detailed below, the samples of known hydration state were prepared and measured; the parent material in this case was the hexahydrate. For both the parent and daughter products, sample identity was confirmed using x-ray diffraction patterns as the "ground truth" method. The transformation was also observed using other experimental techniques such as microscopy, but also theoretical methods, namely *ab intio* chemical colocations using Density Functional Theory (DFT) to predict geometries and infrared spectra. Details are found below.

2. EXPERIMENTAL

Infrared spectroscopy has been used for decades both as an analytical technique to identify materials and also as a tool of chemical physics to probe the nature and strength of chemical bonds. In the early years this involved primarily transmission measurements where the sample of interest was prepared as a dilute component in an infrared transparent medium such as Nujol mull or more commonly pressed into an alkali halide pellet such as NaCl or KBr. Such techniques are cumbersome, time-consuming, and do not allow for dynamic studies of materials as the analyte is "frozen" in the mull or salt matrix. However, in the case of the uranyl nitrate hydrates, the method also suffers from the fact that the sample preparation can affect the state of hydration. As the salts are anhydrous, they can remove waters molecules from the species of interest; even the act of grinding or powdering the sample can desiccate the material. In other cases, for both organic and inorganic salts the ions can metathesize with those of the NaCl or KBr matrix. Hence, the primary method used in our studies is infrared reflectance spectroscopy. While the spectra are more complicated to interpret than simple transmission spectra, no sample preparation (or alteration) is required, and dynamic studies are more easily accomplished.

2.1 Infrared Spectroscopy

The system used here is a Bruker Matrix/M IRCube spectrometer that provides a modulated IR beam output that is directed into the horizontal entrance port of an A562 integrating sphere, which is permanently bolted to the Matrix. The Matrix spectrometer is equipped with a glow bar source, a KBr beamsplitter and an external detector electronic input for the mid-band MCT detector (2 x 2 mm element) which is attached to the A562 as seen below. The A562 is a two-port 75 mm diameter gold-coated integrating sphere with a baffled detector optic and three sphere ports. The sample or a reference material sits at the bottom port; a mirror on a lever arm can be used to direct the incoming horizontal light beam from the FTIR either down towards this sample position, or upwards to a beam exit port, or to a position on the sphere's front wall, just below the light entrance port.[ref]

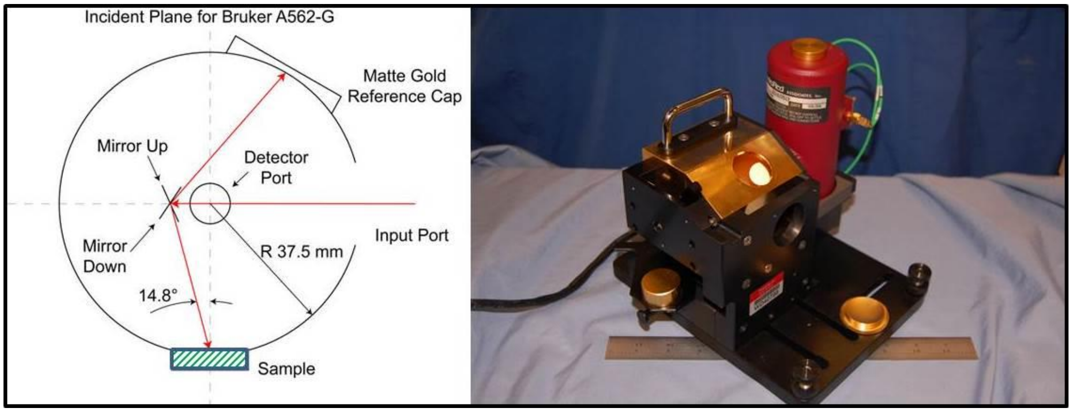

Figure 1. Schematic drawing (left) and photograph of the A562 integrating sphere with infrared detector attached.

As seen at left in Figure 1, with the mirror pointing down towards the sample port, the angle between the incident light on the sample surface and the surface normal is 14.8°. Via use of the upper specular exclusion port with removable dome cap, two sets of spectra can be recorded for each sample: either the diffuse-only reflectance spectra (cap removed) or the total (also called hemispherical) reflectance spectra. The total reflectance measurement captures both the diffuse and specular components that are scattered into the 2π steradians of a hemisphere.[LES, TAB, TLM] For this paper the plots all represent the total hemispherical spectra. The experiment places a few grams of solid powder into an open 1.9-cm diameter sample cup at the bottom of the sphere. Spectra are ratioed relative to a spectrum that also has sample in the cup (for constant sphere albedo). Specifically, the hemispherical spectral reflectance is determined by ratioing the sample spectrum (mirror pointing towards the sample in the bottom port), to a reference spectrum, which is obtained by pointing the beam at the diffuse gold dome located at the top of the sphere, the dome designed to have same curvature as the sphere. For the time-resolved reflectance IR studies we employed our recently developed system that records the directional-hemispherical infrared reflectance spectra. Results are then reported as %R reflectance. The integrating sphere also contains a gas inlet port for purging the sphere, and in this case was fed with an N_2 gas of very low and controlled humidity that was used to desiccate the sample. Interferograms were recorded at 4.0 cm^{-1} resolution in time-resolved fashion at 1.0 minute intervals using Bruker's OPUS 6.5 software; for each spectrum 200 interferograms were averaged before the next one-minute interval acquisition was initiated.

2.2 X-Ray Diffraction Patterns and Optical Microscopy

In order to verify both the chemical and morphological changes associated with the samples during the time-resolved experiment, it was necessary to use additional analytical techniques. We employed both optical microscopy and X-ray diffraction patterns to this end. In terms of XRD, the structures and patterns of the di-, tri- and hexa-hydrate salts of uranyl nitrate are all known and reported.[refs] We therefore analyzed samples before and after using a Rigaku/Ultima IV X-ray Diffraction system equipped with a silicon linear position sensitive detector and graphite monochromated copper X-ray tube (Kα radiation, $\lambda = 1.5406$ Å). Diffraction data were collected from 5° to 90° 2θ with a step size of 0.02 and a scan speed of 3° per minute. Full pattern Rietveld refinements used extract the relative weight percentages of the different uranyl nitrate phases present in each sample were conducted using the TOPAS (Bruker) software package. A hermetically sealed sample holder was used to maintain the hydration state of the uranyl nitrate phase formed while diffraction data were collected. In addition, microscopic studies of the changes were also performed using a Nikon 400POL Polarizing Light microscope equipped with an ARC-2 Paxcam digital camera. Images were obtained automatically over various stages of desiccation. Length scale was calibrated with a National Institute of Standards and Technology (NIST)-2800 microscopy standard.

2.3 Theoretical Chemistry Methods

Modern computational chemistry can help provide several answers to better understand observed physical phenomena, specifically observables such as crystal packing groups, thermodynamic properties [ref] and spectroscopic observables such as vibrational frequencies and intensities. For this project we conducted first-principles total energy calculations using the spin-polarized density functional theory (DFT), as implemented in the Vienna *ab initio* simulation package (VASP). The exchange-correlation energy was calculated using the generalized gradient approximation (GGA), with the parameterization of Perdew and Wang (PW91). The PW91 functional was found in previous studies to correctly describe the geometric parameters and properties of various uranium-containing structures. Although theoretical approaches that go beyond standard DFT are needed to account for the strong on-site Coulomb repulsion between U 5f electrons in bulk UO_2, previous studies on uranyl peroxide phases and uranyl-organic coordination compounds by Weck et al. showed that standard DFT is appropriate to describe the uranyl nitrate systems in this study. Interactions between valence electrons and ionic cores were described by the projector augmented wave (PAW) method. The U(6s,6p,6d,5f,7s), O(2s,2p) and N(2s,2p) electrons were treated explicitly as valence electrons in the Kohn-Sham (KS) equations and the remaining core electrons together with the nuclei were represented by PAW pseudo-potentials. The KS equations were solved using the blocked Davidson iterative matrix diagonalization scheme followed by the residual vector minimization method. The plane-wave cutoff energy for the electronic wavefunctions was set to a value of 500 eV, ensuring the total energy of the system to be converged to within 1 meV per atom.

Figure 2. Photograph of the parent UNH crystals.

3. RESULTS AND DISCUSSION

The uranyl nitrate starting sample display as lustrous lime green crystals as seen above in Figure 2. Besides visual inspection, the hexahydrate form of the starting material was confirmed as pure UNH using x-ray diffraction methods as described earlier. For the infrared experiments, the crystals were placed in an IR sample cup and the phase changed studied further as detailed below. After the infrared experiments, the specimen was found to be almost fully converted, with the XRD results showing the material near fully dehydrated converted to the trihydrate: 84% UNT, 16% UNH. In addition to IR and XRD analyses, the phase transformation was also studied in separate experiment using optical microscopy to show the recrystallization of the UNT from UNH: Figure 3 shows *in situ* polarized light microscopy images of the sample during the process. As the UNH was allowed to precipitate from the uranyl nitrate liquor, it gradually started to dehydrate. The rate of the dehydration was dependent on the RH as also observed in the IR experiments below. The recrystallization was pseudomorphic, in other words, the trihydrate formed within the existing hexahydrate crystals. The crystallite size was far smaller than the original $UO_2(NO_3)_2(H_2O)_6$. This morphological transformation likely accounts for the dull appearance of the UNT relative to the luster of the $UO_2(NO_3)_2(H_2O)_6$ crystals seen in Fig. 2. The loss of water from the structure results in an irreversible transformation.

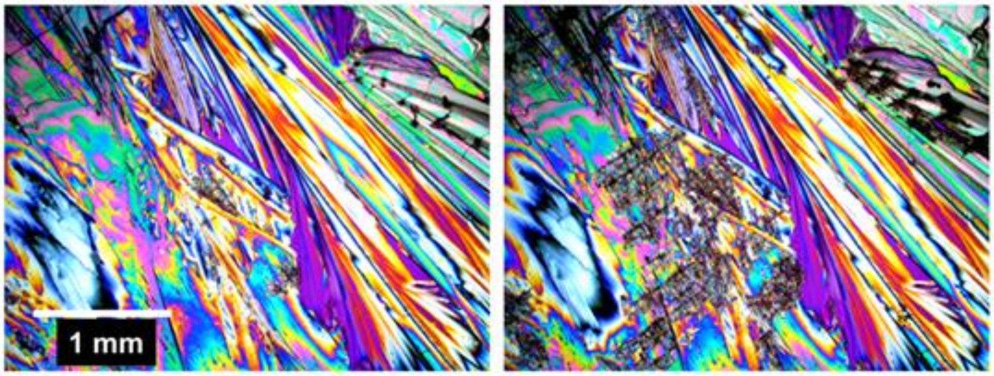

Figure 3. Rapid transformation of uranyl hexahydrate to the trihydrate as observed in the optical microscope.

For the infrared experiments, the uranyl nitrate starting product crystals were loaded into the sample cup, placed at the bottom of the A562 sphere and a reference spectrum (pointing the mirror at the top dome) was recorded over a few minutes time. The time-resolved acquisition was then started such that 200 interferograms were averaged (requiring slightly less than 60 s), and at exactly one minute intervals the next acquisition was started. Interferograms were all transformed to single-beam reflectance spectra at the conclusion of the experiment. There was one ~11 minute gap in the middle where software collection stopped and had to be re-started. Total acquisition time from start to finish was approximately 2.7 hours, and in most cases the peak evolutions showed time-scales of transformation from several minutes to tens of minutes, with similar evolution times for most bands.

While the present method of reflectance spectroscopy has many large advantages (no sample preparation, allowing for dynamic experiments, etc.), understanding the data is slightly more complicated as compared to e.g. IR transmission spectra. The peak amplitudes are not directly proportional to path length or concentration as in Beer-Lambert absorption studies. Indeed, some peaks such as reststrahlen or transparence peaks are upward doing in the infrared, often associate with surface scattering, whereas other peaks tend to be downward-going, associated often with volume scattering phenomena. In the case of relatively weak absorbers diluted in transparent solid media where volume scattering dominates, it is possible to use the Kubelka-Munk relation to estimate relative concentrations, but this relationship is both more complicated than Beer's law, and more limited in applicability. On the wavelength axis, even the peak positions observed in reflectance cannot necessarily be directly compared the positions of absorption and reflectance peak positions as reflectance bands involve both the real as well as the imaginary component of the refractive index, whereas for absorption bands it is only the imaginary component that gives rise to the signal.

In general, in the visible and shortwave infrared surface scattering tends to dominate reflectance spectra of Lambertian samples which show high %R values for small particles when there are no or few absorption bands present. When there are weak to medium absorption bands (i.e. with small buy non-zero k values) they usually manifest themselves as downward-going peaks due to light extinction. Especially in the longwave infrared, however, there can be exceptions to this due to certain phenomena known as reststrahlen bands: These are characterized by large values for both the optical constants n and k, and typically result in surface scattering of the light which manifests itself as upward-going peaks. For many different types of powders where volume scattering dominates, such reflectance spectra tend to be strongly particle-size dependent; smaller particle sizes result in higher albedo, i.e. higher overall reflectivity.

Two of the resulting spectra from our infrared experiment are seen below in Figure 4. In the short- and mid-wave infrared between 6,000 and 1,600 cm^{-1} (not plotted) the overall reflectivity generally showed a simple increase as a function of time. We attribute this reflectivity increase to the UNH sample being desiccated by the dry N_2 purge over a course of ~2 hours, resulting in the formation of the trihydrate with water vapor escaping from the cell.

$$UO_2(NO_3)_2(H_2O)_6 \xrightarrow[N_2(g)]{} UO_2(NO_3)_2(H_2O)_3 + 3\ H_2O\ (g) \qquad (1)$$

Visibly, the product displayed as a matte light yellow-green powder due to the dehydration process. As demonstrated by the polarized microcopy experiments, this is in fact a pseudomorphic recrystallization with a change of both space group and chemical composition. The trihydrate was formed within the existing hexahydrate crystals with the crystallite size being far smaller than in the $UO_2(NO_3)_2(H_2O)_6$ parent complex.

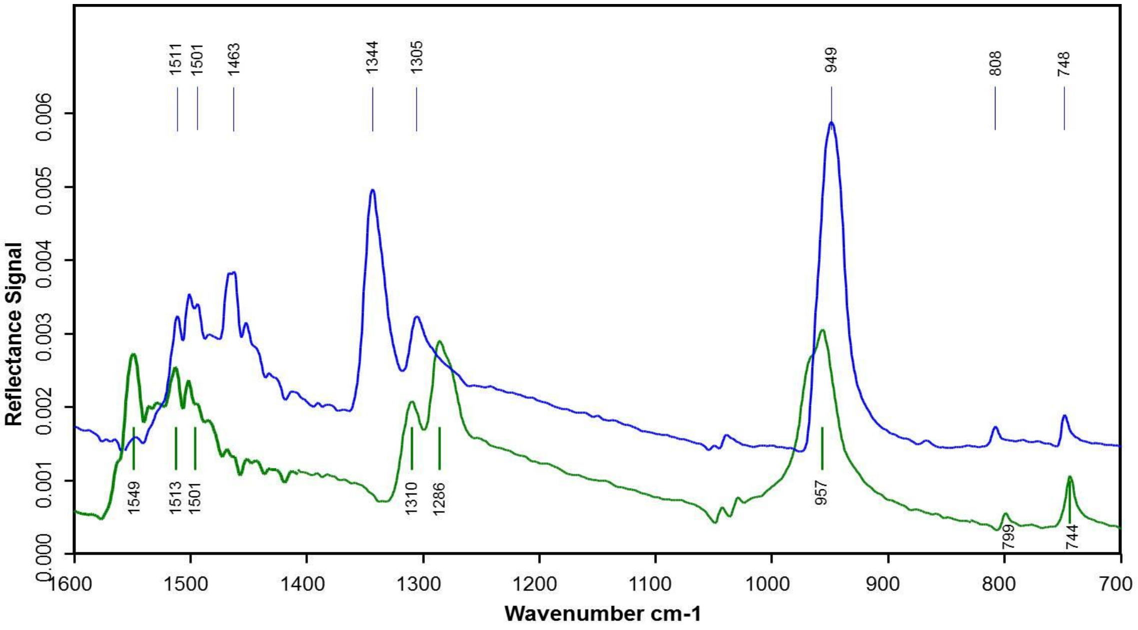

Figure 4. Transformation of uranyl hexahydrate to the trihydrate as observed by reflectance infrared spectroscopy. The starting material (UNH) reflectance spectrum is the blue trace at top, the resulting material (84% UNT, 16% UNH) is the green trace at bottom. The peak labels are as indicated, assuming upward going peaks as seen for reststrahlen-type bands.

Reflectance spectra are more complicated to interpret than IR transmission spectra. At this point we have not completed our full vibrational analysis of these species, but preliminary observations can be made for the “before” and “after” spectra of Figure 4, i.e. for the UNH vs. UNT spectra, respectively. We implicitly assume for the analysis that in this general region of low reflectivity (1600 to 700 cm^{-1}) that the prominent mechanism of light interaction with the materials arises from surface scattering and that the band positions are to be interpreted as upward-going peaks. These observation jive with what has been observed for the peak positions as seen in transmission, but also with the frequencies as predicted by the DFT calculations. One of these frequencies observed in the earliest time-slice spectra (seen at 949 cm^{-1}) is an upward-going reststrahlen peak which we ascribe to the ν_3 band of the asymmetric uranyl stretch of the parent hexahydrate. The same UO_2^{2+} infrared band has been observed in transmission for similar (but not exact) frequencies many decades ago and ascribed to UNH Similar frequencies for the asymmetric uranyl stretch have also been observed and ascribed for many analogous uranyl salts and complexes by other reserarvhers. The reflectance band is typical for a reststrahlen band in that it displays quite a large reflectivity. This is often seen for bands with strong absorption features. The peak shifts to shorter wavelengths and broadens as the sample changes from UNH to UNT: The uranyl reflectance peak first grows in as shoulder on the high energy side, and ultimately forms a doublet band with reflectance peaks at 966 and 957 cm^{-1} as seen in the figure. These changes and assignment, particularly of the UO_2^{2+} splitting are consistent with known crystallography: In the hexahydrate the UO_2^{2+} cations all occupy equivalent positions in the orthorhombic $Cmc2_1$ space group. In in the triclinic space group $P\bar{1}$ for UNT there are two distinct (inequivalent) unit cell positions for the uranyl cation resulting in the two IR frequencies.

While it is not strictly correct to compare intensities between infrared reflectance spectra vs. the DFT-predicted absorption spectra, the DFT-calculated frequencies and their relative intensities and trends can be quite useful. For example, for the asymmetric uranyl stretch the trend suggested by the DFT theory matches fairly well what is seen in experiment: Upon dehydration of the hexahydrate to the trihydrate, the O=U=O asymmetric stretch splits due to the lower symmetry, with the two resultant bands shifting to frequencies +2 and +10 cm^{-1} higher as predicted by DFT. The changes are comparable to what is observed for the experimental reflectance with shifts of +8 and +17 cm^{-1} from the parent UNH reststrahlen band at 949 cm^{-1}.

Also seen in Figure 4 are several IR reflectance band in the 1200 to 1600 cm-1 range. The DFT predicted frequencies differ from the experimental values by approximately 3% in the 1200 – 1600 cm^{-1} domain in general, but can still be used to assign many of these modes: As one example, for the parent UNH molecule (blue trace in Figure 4), the reflectance band observed at 1305 cm^{-1} was predicted at 1278 cm^{-1} (in absorption) by DFT as a NO_3^- ion twist coupled with OH wagging in equatorial water molecules. As the compound transforms to the trihydrate, the reflectance bands observed at 1286 and 1310 cm^{-1} (green trace) are assigned using DFT results and are predicted to occur at 1225 and 1274 cm^{-1} and are assigned, respectively, to the NO_3^- twisting bound to U_1 and the NO_3^- twisting bound to U_2 where to U_1 and to U_2 are the inequivalent uranium atoms in the triclinic space group of the trihydrate product. That is to say, due to the inequivalency of the two uranyl groups and the changed local environment the normal mode at 1225 cm^{-1} is attributed to twisting of nitrate ligands connected to U_1 whereas the mode at 1274 is due to twisting of the nitrate ligands connected to U_2. Further assignments using the DFT results and previous literature values are currently being undertaken.

4. SUMMARY

We have observed the dehydration of uranyl nitrate hexahydrate to uranyl nitrate trihydrate under ambient conditions using a new method. Rather than traditional infrared transmission methods, we have used infrared reflectance spectroscopy which allows for dynamic observation of the infrared spectrum. The uranyl nitrate starting sample display as lustrous lime green crystals as seen in Figure 2, but transformed to the matte yellow-green materials of the trihydrate. Besides visual inspection, the hexahydrate to trihydrate transformation was confirmed using both x-ray diffraction and and also polarized optical microcopy to monitor the change. We note that in the transformation of the uranyl hexahydrate to the trihydrate neither heat nor chemical reagents were applied to effect the transformation, other than flowing (nitrogen) air of lower humidity as seen in Equation (1).

Our results indicated that the uarnyly nitrate hexahydrate that first precipates from aqueous solution clearly undergoes a chemical reaction and phase transformation to the trihydrate, losing three water molecules from each unit cell. Certain results indicate that extremely low humidity the dihydrate is formed. We suspect and have made preliminary investigations into the hyptothesis that many of the IR transmission measurements made in the past using either Nujol mulls or KBr pellets have in fact ended up converting any UNH sample into the trihydrate due to either the mulling/powdering processes, the use of KBr, etc. Preliminary experiments have shown that unless the RH is kept high, the material dehydrates. This obviously has strong effects on those normal modes that invove water molecule bending, torsion etc. Other results indicate that there may also be methathesis reactions that occur as the pellet is formed. The reflectance method does not suffer from such proabitve effects and further allows montiroging of the sample during the course of ther eaction. Fursther exepriments to investigate this are planned.

Sandia National Laboratories is a multi-program laboratory managed and operated by Sandia Corporation, a wholly owned subsidiary of Lockheed Martin Corporation, for the U.S. Department of Energy’s National Nuclear Security Administration under contract DE-AC04-94AL85000.